Comparison of H^+ and He^+ plasmapause locations based on resurrected and reevaluated OGO-5 ion composition data base

Vladimir Truhlik[1] , Ludmila Triskova[2] , Robert F. Benson[3] , Dieter Bilitza[4,5], Joseph Grebowsky[6] , Phil G. Richards[7], and Jan Smilauer[8]

[1]Institute of Atmospheric Physics, Acad. Sci. Czech. Rep., Prague, Czech Republic, vtr@ufa.cas.cz

[2]Institute of Atmospheric Physics, Acad. Sci. Czech. Rep., Prague, Czech Republic, ltr@ufa.cas.cz

[3]Geospace Physics Laboratory, Code 673, Heliophysics Science Division, Goddard Space Flight Center, Greenbelt, MD 20771, USA

[4]George Mason University, School of Physics Astronomy and Computational Science, 4400 University Drive, Fairfax, Virginia, USA,dbilitza@gmu.edu
[5]NASA Goddard Space Flight Center, Heliospheric Physics Laboratory, Greenbelt, Maryland, USA, dieter.bilitza-1@nasa.gov

[6]Planetary Magnetospheres Laboratory, Code 695, Solar System Exploration Division, Goddard Space Flight Center, Greenbelt, MD 20771, USA

[7]George Mason University, School of Physics Astronomy and Computational Science, 4400 University Drive, Fairfax, Virginia, USA,dbilitza@gmu.edu, prichar1@gmu.ede

[8]Institute of Atmospheric Physics, Acad. Sci. Czech. Rep., Prague, Czech Republic, jsm@ufa.cas.cz

ABSTRACT

Orbiting Geophysical Observatory 5 (OGO 5) magnetospheric ion-composition data (H^+, He^+ and O^+) from an ion spectrometer (Sharp, 1969) have been retrieved from old magnetic tapes archived at the National Space Science Data Center (NSSDC). The highly compressed binary format was converted into a user-friendly ASCII format and these data have been made available online. We have inspected reliability and consistency of this data set in state of the art current knowledge. Comparing with the climatological model IRI-2012 and the mathematical model FLIP a shift of absolute and relative ion densities with time was revealed. We have suggested a correction procedure of individual H^+, He^+ and O^+ ion densities. Using the corrected data set, we investigated plasmapause locations based on density gradient in H^+, and He^+. Correlation coefficient of both locations was determined as ~0.886 and the typical difference $\Delta L \sim 0.1$. The electron density at the He^+ plasmapause location for all cases is >100 cm^{-3}.

KEYWORDS: Plasmasphere,Plasmapause, FLIP, Empirical model, OGO-5

1. Introduction

The plasmasphere with its outer boundary plasmapause intensively attracted scientific attention shortly after its discovery more than sixty years ago (Storey, 1953). The plasmasphere is a region of the magnetosphere filled with charged particles of ionospheric origin with the energy of less than 1-2 eV which are trapped on geomagnetic field lines. It reaches to the equatorial geocentric distance of several Earth radii depending on geomagnetic conditions. The plasmapause is a field aligned surface forming the outer boundary of the plasmasphere and is characterized by a sharp decrease of the particle density; a drop by a factor of 5 or more within the increase of L by 0.5. The plasmasphere and plasmapause, their configurations, dynamics, refilling and dependence on magnetic activity were subject of numerous studies based on the space probe, ground based observations and numerical models (e.g.Chappell et al., 1970; Carpenter and Anderson, 1992; Decreau et al., 1986, Goldstein et al., 2004, Kotova et al., 2008, Pierrard et al., 2009, Darrouzet et al., 2009a, Darrouzet and Keyser, 2012; Krall and Huba, 2013). Also monographs on the plasmasphere were published by Lemair and Gringauz, 1986 and by Darrouzet et al. 2009b.

The location of the plasmapause was defined using the electron density (N_e) since this parameter is of primary interest and is detected in most experiments (plasma probes, whistler, radio soundings). Later, using mass spectrometer measurements it was found that the plamasphere consists of majority of H^+, with some fractions of He^+, and even heavier ions as O^+, N^+, O^{++} etc. (Horwitz et al., 1986; Craven et al., 1997). Considerable interest on He^+ in the plasmaspere rose the possibility of detection of this ion using EUV 30.4nm He^+ which brought plasmaspheric research on a new level employing EUV imaging (Sandel et al. 2003). However, possible differences between location of the plasmapause boundary determined from N_e ($\sim N_{H^+}$) and He^+ were outside of the interest. Recently Obana et al. (2010) dealt with such a problem. Using plasmapause location inferred from ground-based magnetometers (mass density determined from the eigenfrequency of field line resonance in the ULF band) and near simultaneous plasmapause locations from EUV images obtained by the IMAGE and the Kaguya satellites they found in 18 from 19 cases that the He^+ plasmapause and mass density plasmapause were detected at the same L-shell with an error of ~0.4L. Only one case showed a larger difference probably caused by the state after refilling and by different refilling rates of H^+ and He^+.

In this paper we compare the position of the plasmapause determined from the H^+ and He^+ densities measured onboard the Orbiting Geophysical Observatory 5 (OGO 5) and defined as the L-value of the last point measured prior to the steep density drop (Carpenter and Anderson 1992). OGO-5 data is a unique data base giving the possibility of such a simultaneous comparison and as we know they have never been used for such a purpose. Of course, OGO-5 ion mass spectrometer data served as one of the first and most detailed in-situ measurements for study and revelation of fundamental properties of the plasmasphere and plasmapause (e.g. Chappell et al.1972).

We also report a successful effort to restore these data from old magnetic tapes in the NSSDC archive and make them available online for the scientific community.

2. Experiment and data restoration

The Orbiting Geophysical Observatory 5 (OGO 5) was one of the six OGO satellites launched by the United States on March 4, 1968 designed to study the Earth's magnetosphere. The orbit of OGO-5 was highly elliptical and was changed on January 31, 1969 using an onboard propeller (Table 1).

Table 1
OGO-5 orbit

Epoch	Inclination (i)	Orbital period (P)	Height perigee (h_P)	Height apogee (h_A)
68-03-04.6	31.13°	3795.90 min	232 km	148228 km
69-01-31.3	43.80°	3745.70 min	6045 km	140978 km

Among the 25 experiments onboard the satellite a very sensitive magnetic-focus ion spectrometer was carried which measured the ionic abundance of masses 1, 4, and 16 (Harris and Sharp, 1969). Data are available in the interval from March 7, 1968 to May 31, 1969. This time interval corresponds to the maximum of the 20th solar cycle which is considered as a moderate solar maximum. The F10.7 81-day running average was in the interval from 139 to 164. In the next section we discuss in more detail the data quality and reliability.

The highly compressed binary format from old magnetic types archived at the NSSDC has been recently converted into a user friendly ASCII format and is available online at http://nssdcftp.gsfc.nasa.gov. The data are provided in 45 data files. All data are given in the E12.6 format. Each line/record has 12 parameters: 12(1X,E12.6). A block structure is used to separate the measurements for different ions. The first 500 lines contain the O^+ data, the next 500 lines the He^+ data, followed by 500 lines of H^+ data and starting over again with 500 lines of O^+ data. The separation between the different ion blocks are also marked by a blank line and by a jump backwards in time.

The very first file ogo5_1_001.asc includes a 4-line header which also explains the different parameters. Originally these data were submitted by the PI on magnetic tape. The documents that accompanied this submission are included in this directory as a PDF document (Ogo5_ion_dens_original_submission_document.pdf
ftp://nssdcftp.gsfc.nasa.gov/spacecraft_data/ogo/ogo5/IMS_ion_densities/
Total amount 360,500,808 bytes in 153 files.

3. Data consistency and correction

a) H^+, He^+ and O^+ density measurement vs. time of the mission

We inspected the consistency of the OGO-5 data with special attention to its development during the mission. Figure 1 shows density of H^+, He^+ and O^+ in the altitude range of 9000-9500 km close to the field line L=2.5 vs. universal time (days from January 1, 1968). The upper panel shows density of H^+, middle panel density of He^+ and lower panel density of O^+ by color symbols.

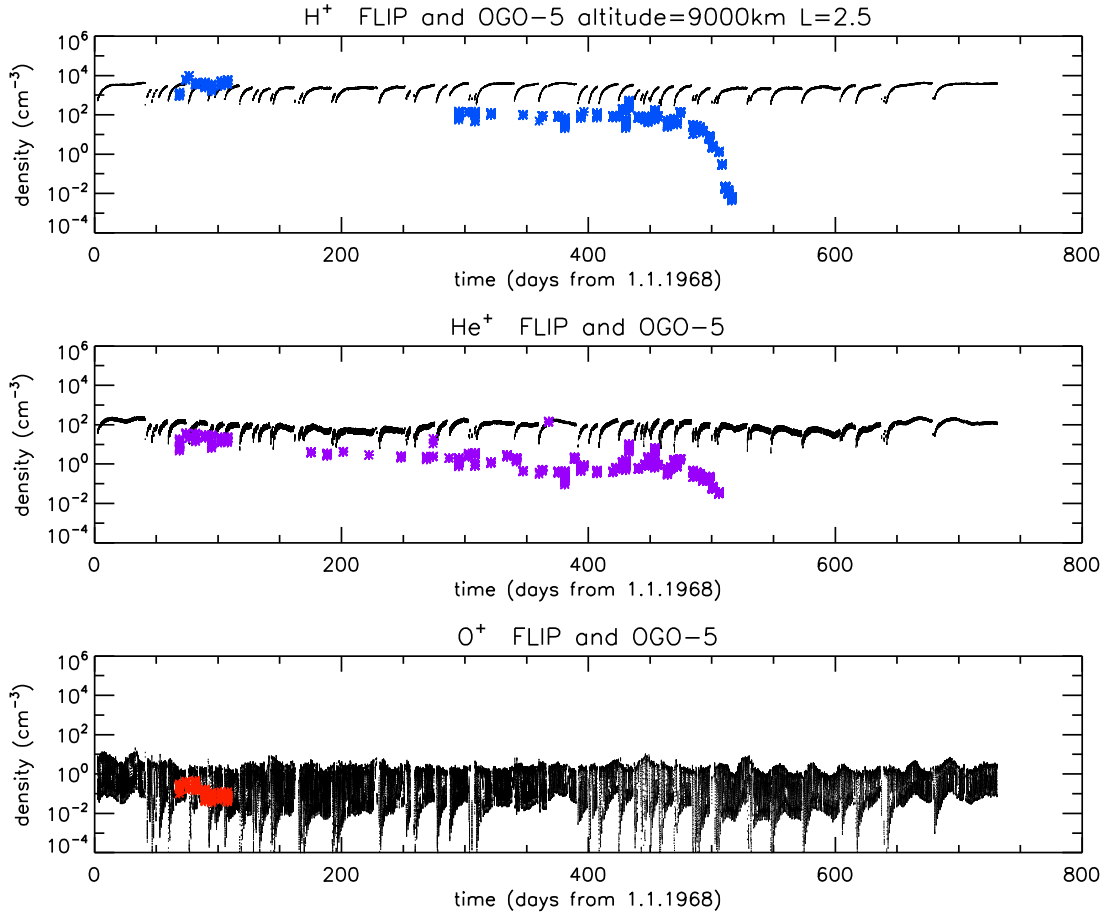

Fig. 1. H^+, He^+ and O^+ density (color symbols) in the altitude range of 9000-9500 km close to the field line L=2.5 vs. universal time (days from January 1, 1968). Black dots – density calculated by the FLIP model. Small "quasi-periodic" discontinuities apparent e.g. on simulated H^+ density is given by geomagnetic disturbances reflected by neutral density (MSIS) model which serves as FLIP input (see the Section 4). The large spread of the calculated O^+ values is caused by the diurnal variation.

For comparison, we added in each panel the density calculated by the FLIP model (Richards, 2001; Richards et al., 2010). It is apparent that the measured H^+ and He^+ are available for almost the whole interval of the mission but the density of O^+ is available only for the first months. This fact indicates a possible problem that occurred with the instrument after April 23, 1968. Another noticeable feature of the measured data is that densities of H^+ and He^+ exhibit some fading in time. This fading is very pronounced close to the end of the interval (sudden decrease of the density of H^+ from about 100 to 0.01). On the other hand, densities of these ions calculated by the FLIP model do not exhibit such a behavior. The model calculation shows that this effect is not caused by variation of geophysical conditions (e.g. the solar or geomagnetic activity).

b) Variation of H^+, He^+ and O^+ with altitude

Another method how to check the data consistency is to plot altitude profiles obtained from averaging the measured values into specific altitude bins for a given field line (L=2.5), and local time (day). Example of such profiles is shown in Figure 2.

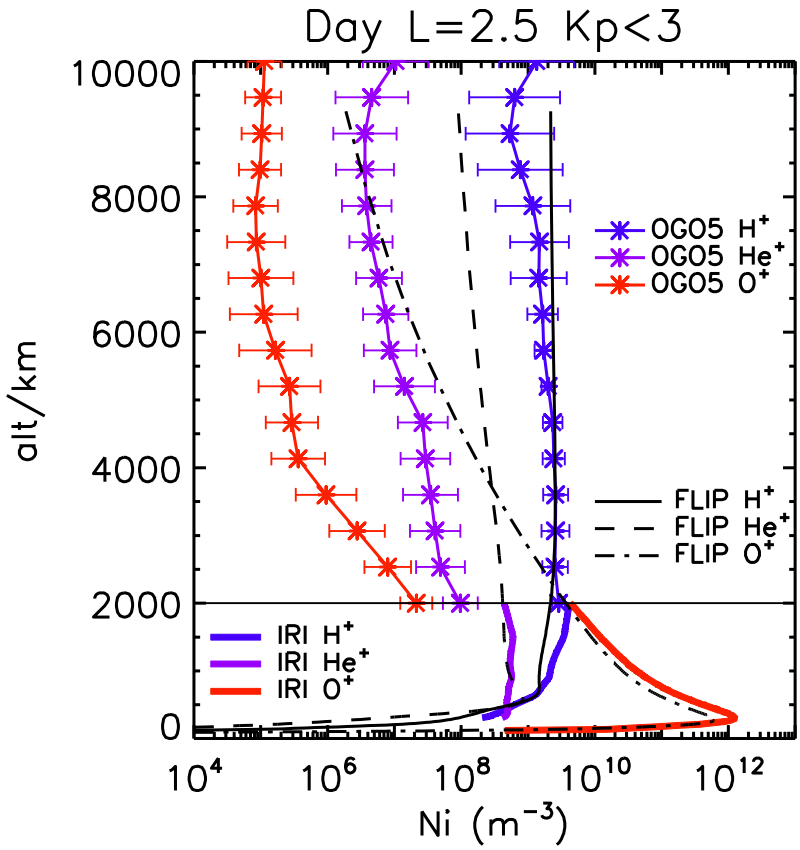

Fig. 2. OGO-5 altitude variation of averaged H^+ (blue), He^+ (magenta) and O^+ (red) densities for day-time (MLT=12h±4h), L=2.5±0.2, and low geomagnetic activity (Kp < 3) between 2000 and 10000 km represented by thin lines with asterisks (data averages), standard deviations plotted by error bars. The plot is completed by IRI 2012 H^+, He^+ and, O^+ from bottomside up to 2000 km (options NeQuick and TTS-03 for MLT=12h, March 21, 1968, glat=38°, glon=285°) by thick color lines. FLIP values are showen for the whole altitude range by black lines (H^+ solid, He^+ dashed and O^+ dash dot). The FLIP data were selected from MLT=12h±4h, L=2.5, and low geomagnetic activity (Kp < 3).

It shows altitude variation of the H^+, He^+, and O^+ densities as measured onboard the OGO-5 satellite at a fixed local time and field line under low geomagnetic activity. For comparison we have also plotted density calculated by the IRI 2012 model (colored lines from ionospheric altitudes up to 2000 km) and density from the FLIP model (black continuous lines from ionospheric altitudes up to about 9000km). It is apparent that the H+ density from OGO-5 agrees quite well with the FLIP model in the plasmasphere and with the IRI-2012 model in the topside ionsophere. Note that FLIP agrees quite well with IRI in the topside ionsophere for all three ions (there are some minor differences but they are behind the scope of this study). However, densities of He^+ and O^+ show a large depart from densities calculated by IRI at 2000 km and from densities obtained from FLIP in the plasmaspheric heights.

Findings from the analysis of Figures 1 and 2 can be interpreted as an instrumental problem. Therefore we propose a correction which can in some extend solve it.

c) Correction of OGO-5 ion mass spectrometer measurement

We have suggested correction coefficients for measured values of the H^+, He^+ and O^+ densities. These coefficients are based on rations between OGO-5 data and values from IRI

and FLIP models. They were calculated at two UT intervals. Data from the end of the measurement after April 14, 1969 were removed completely.

Table 2.
Correction coefficients

ion	time period	coefficient
H^+	March 7, 1968 ... Apr 23, 1968	1.010
	Apr 24, 1968 ... April 14, 1969	14.81
He^+	March 7, 1968 ... Apr 23, 1968	2.688
	Apr 24, 1968 ... April 14, 1969	16.86
O^+	March 7, 1968 ... Apr 23, 1968	202.0
	Apr 24, 1968 ... April 14, 1969	no data

The coefficients (Table 2) were used to correct ion densities measured by the ion mass spectrometer. The result can be seen in Figures 3 and 4**.** It is apparent that the corrected experimental profiles are in a good agreement with both modes (IRI and FLIP).

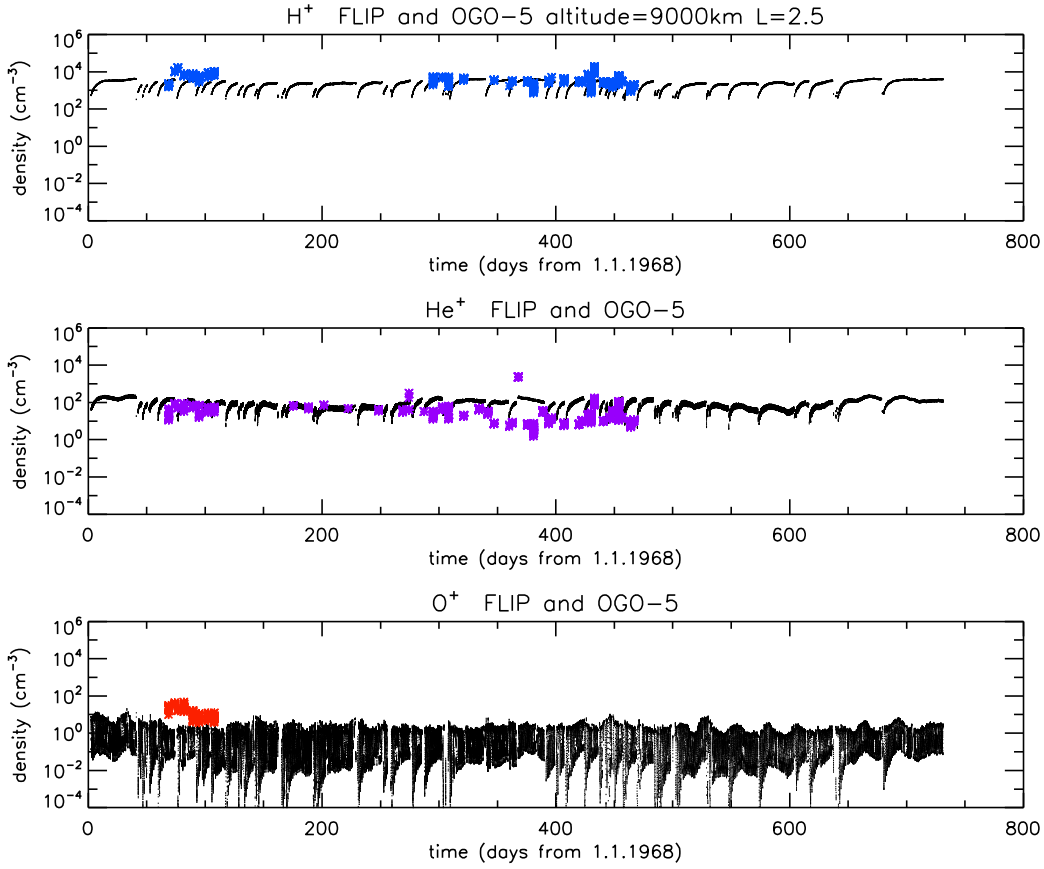

Fig. 3. H^+, He^+ and O^+ densities (color symbols) in the altitude range of 9000-9500 km close to the field line L=2.5 vs. universal time like in Figure 1, corrected using constants from Table 2. Dots – density calculated by the FLIP model.

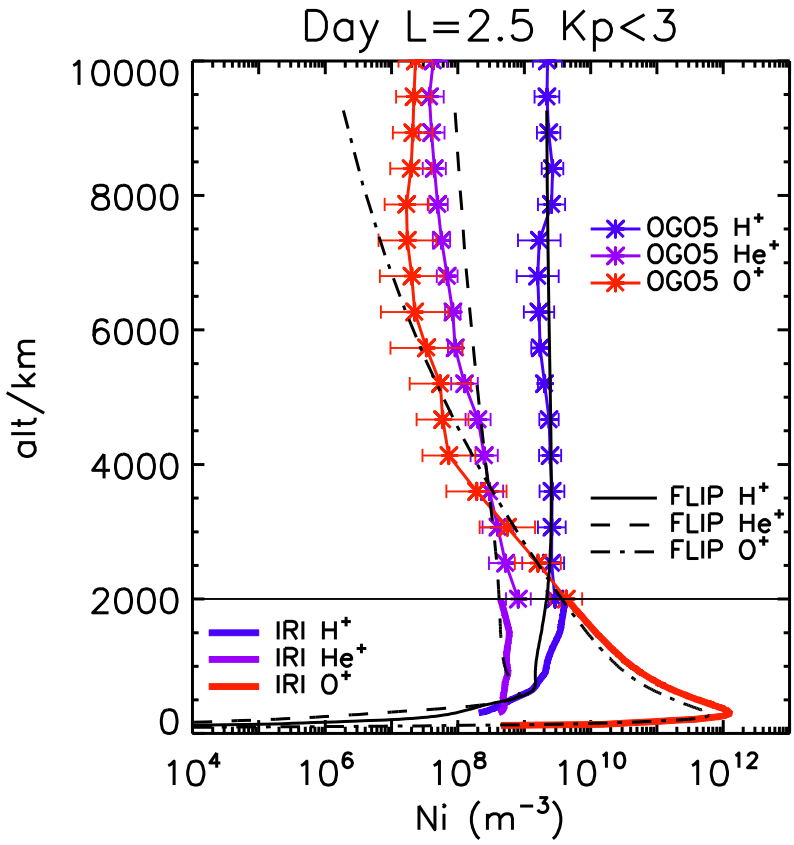

Fig. 4. The same as Figure 2 except OGO-5 data were corrected using coefficients from Table 2. The agreement between data and models substantially improved.

4. Models used for data correction

4.1. FLIP

The field line interhemispheric plasma (FLIP) model is a one-dimensional (1-D) model that calculates the plasma densities and temperatures along entire magnetic flux tubes from below 100 km in the Northern hemisphere through the plasmasphere to below 100 km in the Southern hemisphere. The model uses a tilted dipole approximation to the Earth's magnetic field (Richards, 2001; Richards et al., 2010). The equations solved are the continuity and momentum equations for O^+, H^+, He^+ , and N^+ and the energy equations for ion and electron temperatures. The equations are solved using a flux-preserving formulation together with a Newton iterative procedure that has been described by Torr et al. (1995). Electron heating due to photoelectrons is provided by a solution of the two-stream photoelectron flux equations using the method of Nagy and Banks (1970). The photoelectron solutions have been extended to encompass the entire field line on the same spatial grid as the ion continuity and momentum equations. Chemical equilibrium densities are obtained for NO^+, O_2^+, N_2^+, $O^+(2P)$, and $O^+(2D)$ ions below 500 km altitude in each hemisphere. The densities of minor neutral species NO, O(1D), N(2D), and N(4S) are obtained by solving continuity and momentum equations from 100 to 500 km in each hemisphere. The model also has the capability of solving for the first five excited states of vibrationally excited N_2 that can significantly increase the $O^+ + N_2$ reaction rate.

The solar EUV fluxes are important because they are not only responsible for the ionosphere but also for the photoelectrons that heat the thermal electrons. The FLIP model

uses the EUV model for aeronomic calculations (EUVAC) for the solar EUV fluxes (Richards et al., 1994). Richards et al. (2006) showed that the EUVAC model fluxes are consistent with recent satellite measurements. The primary heat source for thermal electrons is the photoelectron flux, which is calculated by the FLIP model from the solar EUV fluxes (Richards et al., 2006). There is an additional source of electron heat from electron quenching of N(2D) (Richards, 1986). The FLIP model ion-neutral cooling rates are from Schunk and Nagy (1978). The 3 main cooling processes of thermal electrons are (1) Coulomb collisions with ions, (2) fine structure excitation of atomic oxygen, and (3) vibrational excitation of N_2. There is cooling by vibrational excitation of O_2 as well as rotational excitation of O_2 and N_2 and excitation of O(1D) but these are minor above 250 km. The FLIP model electron- ion cooling rate is from Itikawa (1975). For this study the model chemical reaction rates have been updated to those published by Fox and Sung (2001). For the neutral atmosphere the FLIP model uses the revised MSIS model, NRL Mass Spectrometer, Incoherent Scatter Radar Extended model (NRLMSISE-00) (Picone et al., 2002). The NRLMSISE-00 model O_2 densities are not much different at solar minimum but they are a factor of 2 smaller than in previous MSIS models (Hedin, 1987) at solar maximum. Recently the FLIP model was improved by inclusion of the E × B drift which is employed for studies at equatorial, low and high latitudes.

For this study the FLIP model was run for the conditions as follows:
-time from January 1, 1968 to December 31, 1969
-mid-latitude flux tube L=2.5 for the longitude sector of Wallops Island.

This L=2.5 field line was chosen as a typical plasmaspheric L-shell. The plasmasphere at this L shell is not very often affected by geomagnetic disturbances. According to the relation $Lpp=5.6-0.46*Kp_{max24}$ (Carpenter and Anderson, 1992) only maximum Kp in previous 24 hours greater than 7- can affect this field tube. This occurred only in about 10 days from the interval Mach 1968 - April 1969 what is about 2.5% from the whole interval. Thus, most of the time this flux tube can be considered as fully saturated. This simplify the comparison with FLIP since the model was not run with external electric field pertaining to enhanced magnetospheric convection.

In the simulation the parameter "photoelectron trapping factor" was set as 0.2. No additional heat source was considered. This can result in lower temperatures at higher altitudes (Balan et al. 1996) but the electron density in the equatorial latitude is still in the agreement with the IMAGE/RPI data (Tu et al., 2003).

Wallops Island and the quasi-conjugate station Argentine Island ionosonde data (hmF2) were used as input for calculation of the equivalent winds (Richards, 2001; Bilitza et al., 2007). The model was run with the time resolution about 10 minutes and with the actual t values F10.7 and magnetic activity. For the comparison with the OGO-5 measurements (Figures 2 and 4), calculated data were selected for the same conditions as the measured once.

4.2. IRI-2012

For the calibration of the OGO-5 data the calculations from the FLIP model were completed in the region of the transition between topside ionsophere and lower plasmasphere by the IRI model. The International Reference Ionosphere (IRI) is an empirical standard model of the ionosphere and the topside ionsophere based on available and reliable data sources specifying monthly averages of electron density, ion composition, electron temperature, and ion temperature in the altitude range from 50 km to 2000 km (Bilitza et al., 2008; Bilitza et al., 2011). In the present paper NeQuick as the recommended IRI option for the electron density in the topside ionsophere was used (Radicella, 2009).

For the ion composition a model developed by Triskova et al. (2003) which is included in IRI as the recommended option since IRI-2007 was employed. This newer model takes advantage of better global coverage provided by satellite ion mass spectrometer measurements (Interkosmos-24, AE-C, AE-E) and uses the invdip latitude coordinate that is close to the magnetic inclination (dip) near the magnetic equator and closer to invariant latitude at higher latitudes and thus correlates well with the observed variation patterns of the topside ions (Truhlik et al., 2004).

5. H^+ and He^+ plasmapause locations resulting from the corrected data

The calibrated densities of H^+ and He^+ were plotted for individual orbits in the dependence on the McIlwain L parameter. All the plots were inspected. The inspection was made independently for H^+ and He^+. We could identify 97 plasmapause crossings in H^+ and 59 in He^+. At the same time 48 plasmapause crossings in both, H^+ and He^+ were found (Figure 5). As mentioned above, in this paper the position of the plasmapause is defined as the L-value of the last measured point prior to a steep fall of the plasma density (e.g.Carpenter and Anderson, 1992), i.e. at its high density limit. All identified plasmapause crossings fulfill the gradient limit defined in Carpenter and Anderson (1992). Example for 48 crossings for H^+ see Figure 6. The corresponding gradient in the He^+ plasmapause limit is not shown since He^+ density in the outer plasmapause limit can be under the instrument threshold (~0.1 cm^{-3}).

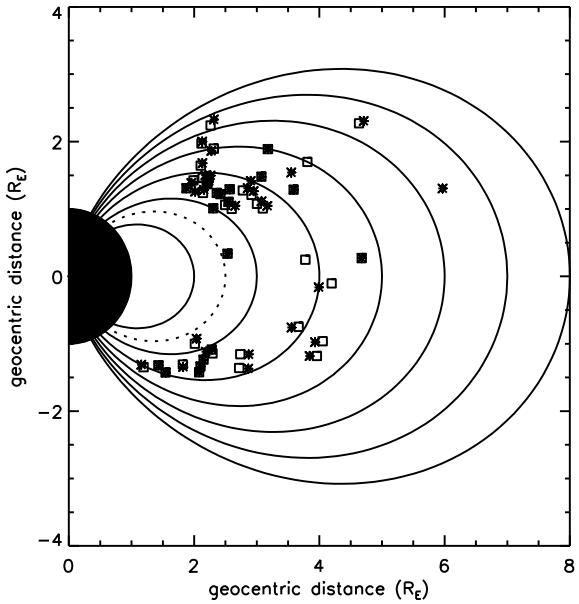

Fig. 5. The 48 identified OGO-5 plasmapause crossings in H^+ (*) for which simultaneous plasmapause crossing in He^+ (□) also exists and plotted in dipolar geomagnetic field.

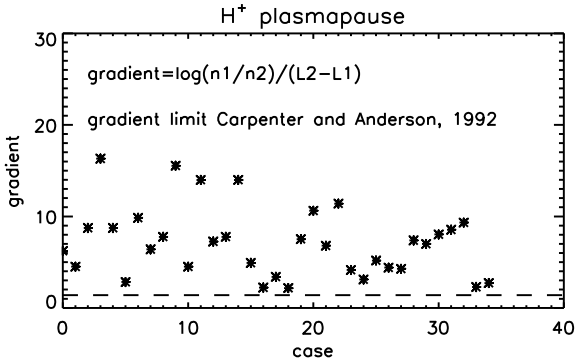

Fig. 6. Gradient of the 48 OGO-5 plasmapause crossings in H^+. All 48 crossings fulfill the gradient limit (dashed line) defined in Carpenter and Anderson (1992).

Figure 7 shows the cross correlation of the plasmapause location in H^+ and He^+. The plasmapause locations in H^+ are plotted on the x-axis and the plasmapause loation in He^+ are plotted on the vertical y-axis. It can be seen that the values are close to the line "y=x" with some exceptions (outliers). The linear Pearson correlation coefficient is 0.886. The most distant outlier, $Lpp(H^+) = 6.4$ and $Lpp(He^+) = 3.8$ belongs to the plasmapause crossing on 9 March 1968 and it will be discussed in the next section.

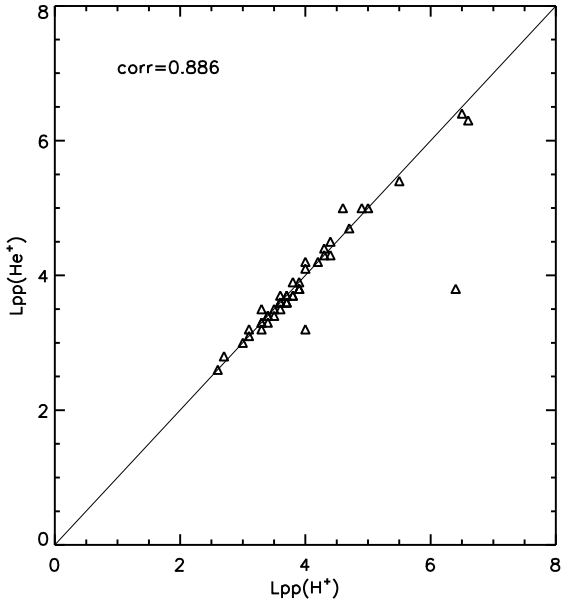

Fig. 7. Cross correlation of the plasmapause locations derived from the OGO-5 H^+ and He^+ density profiles.

Figure 8 shows dependence of the H^+ and He^+ plasmapause locations on the geomagnetic activity. For comparison with results in Carpenter and Anderson (1992) only values from MLT 0-15 h are plotted. As a geomagnetic index, modified Kp_{max24} defined in Carpenter and Anderson (1992) was used (Kp maximum in previous 24 h but in the case of 3-hour periods centered on 09, 12, and 15 MLT, respectively, the Kp values for one, two or three immediately preceding 3-hour period were ignored). In both panels the solid line represents a least square linear fit.

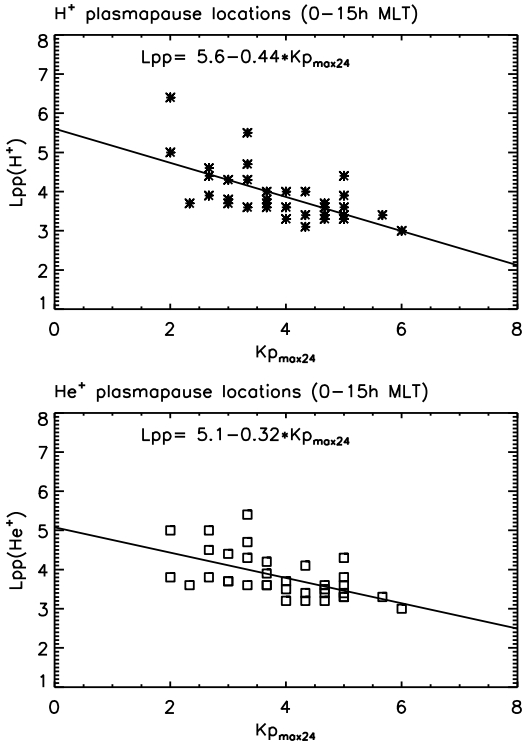

Fig. 8. Dependence of plasmapause locations in H^+ (upper panel) and He^+ (lower panel) on geomagnetic activity and corresponding linear fits. Kp_{max24h} index see the definition in Carpenter and Anderson (1992).

Comparison of both linear fits is shown in Figure 9, where the dependence Lpp=5.6-0.46*Kp_{max24} of the inner plasmapause limit from Carpenter and Anderson (1992) is also plotted. It can be seen that the differences between the linear dependences are typically of the order $\Delta L \sim 0.1$. Maximal differences are in the extremes of the Kp_{max24} index - for its minimum near 0 and large values close to 8 the difference reaches about $\Delta L=0.5$. For the medium geomagnetic activity the statistical differences are negligible.

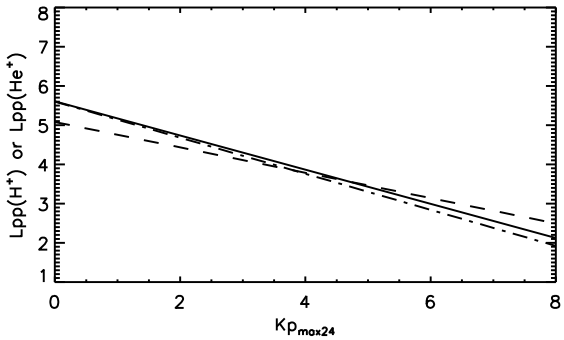

Fig. 9. Comparison of linear fits from Figure 8 (solid line H^+, dashed line He^+). Also added the Lpp=5.6-0.46*Kp_{max24} dependence derived in Carpenter and Anderson (1992) (dash dot line).

Bearing in mind results from Figures 7 and 8 that the location of H^+ and He^+ plasmapauses are in most cases almost identical, we plotted in Figures 10a and 10b the electron density at the plasmapause detected from He^+. The non-corrected OGO-5 data show much lower densities than the corrected ones. This could lead to a misleading conclusion that the too low density at the He^+ plasmapause (detected e.g. by IMAGE EUV imager) in many cases cannot see the plasmapause correctly. However, the corrected OGO-5 data shows that

all cases show the densities significantly above the IMAGE EUV threshold (Goldstein et al., 2004). Of course, not all measured points refer to the equatorial plane (Figure 5). However, according to the theory of plasma distribution along the flux tube (e.g. Angerami and Thomas, 1964), the gradient of the density is small and therefore corresponding equatorial densities are not much lower than the non-equatorial ones (according to Tu et al. 2003, the ratio of the equatorial electron density to the density at about 4000 km is ~0.5 - see the discussion in the next section).

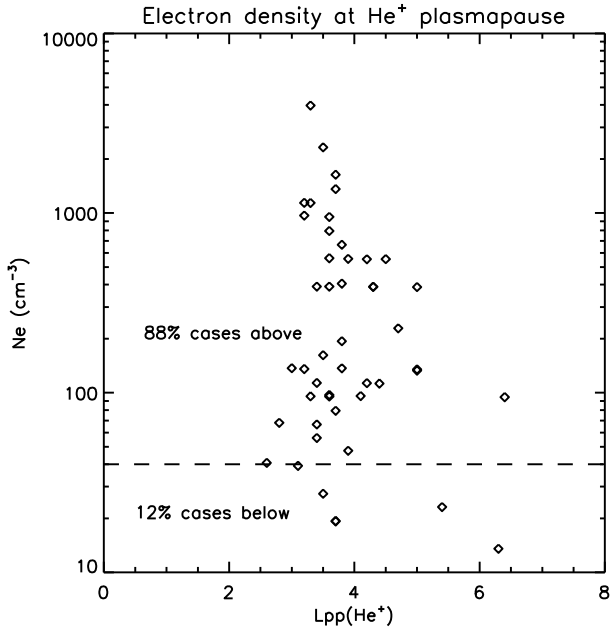

a)

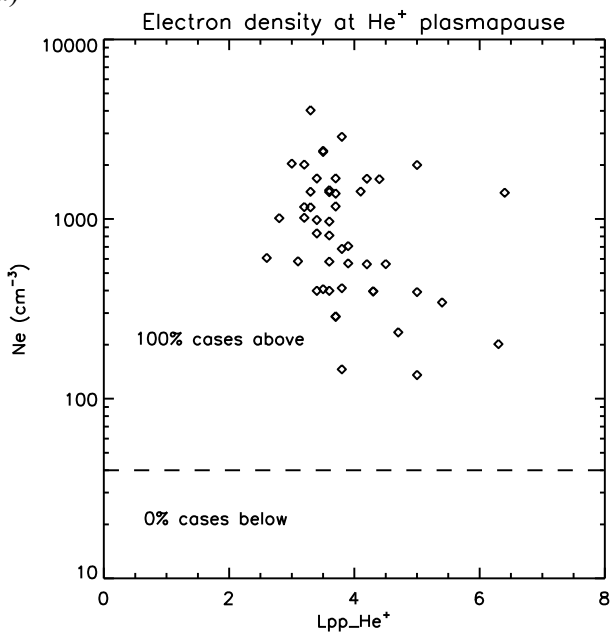

b)

Fig. 10a,b. Electron density at the He^+ plasmapause and IMAGE EUV threshold a) non corrected, b) corrected. For the corrected OGO-5 data, the density in all cases is higher than the IMAGE EUV threshold of 40 el/cm^3 (Goldstein et al., 2004).

6. Discussion and conclusions

The corrected densities of H^+ and He^+ exhibit a better consistency than the original non-corrected values. Especially, the offset and drift in the densities were removed (Figure 3). From Table 2 it follows that the density of H^+ from the commencement of data acquisition until 23 April 1968 almost did not require any calibration since the determined coefficient is 1.01. However, densities of He^+ required correction, the coefficient being 14.81, and the coefficient for O^+ is even 202. After the 23 April 1968 when measurement of O^+ vanished from the data set, H^+ and He^+ required a much higher correction. The correction was based on two models - the climatological IRI model at 2000 km and the mathematical FLIP model in the plasmaspheric height. The IRI model is based on measured and verified data (NeQuick and TTS-03). The consistency of the values from IRI and FLIP in the region of their overlapping in the topside ionosphere (Figures 2 and 4) supports the assumption that the FLIP model values for the plasmasphere are realistic as well. It can be supported by results of other studies. Tu et al. (2003) compared data from IMAGE/RPI with the FLIP model at the field lines L=2.51 and L=3.0. They found a very good agreement on the Equator but the difference increased with decreasing altitude and at about 4000 km the difference was about 40%. The authors concluded that this was a large difference. However, for purposes of our correction this difference is fairly acceptable. From Figure 4 it is apparent that the difference 40% is smaller than the width of the error bars on H^+ and He^+ altitude profiles. Another study (Newberry et al., 1989) compared the He^+/H^+ density ratio from RIMS onboard DE-1 and the FLIP results in the plasmasphere. They found a reasonable agreement between simulations and data. Their ratio varied about 0.2 at 5200 km. Due to different solar activity conditions (peak of strong solar maximum of RIMS DE-1 vs. peak of moderate solar maximum of OGO-5) our corrected data have the He^+/H^+ density ratio about 0.1 at ~5000 km (Figure 2). However, the non-corrected data show the ratio about 0.01 at ~5000 km (Figure 2) which can be considered too low. This is another argument supporting necessity of the OGO-5 data correction.

O^+ as a minor ion in the plasmasphere was not subject to a deeper insight in the frame of this study. In spite of it we showed that the corrected values of the O^+ density up to the altitude of about 6000 km agree with the FLIP simulations and in the topside they almost seamlessly agree with IRI. At higher altitude (>6000 km) where O^+ is a minor ion it seems that the measured density is higher than the FLIP model shows. There are possibilities that O^+ concentration is close to the instrumental threshold or that it decreases with altitude more slowly due to elevated ion temperature. This was observed and described as the heavy ion enhancement in the region close to the plasmapause (Horwitz et al., 1990).

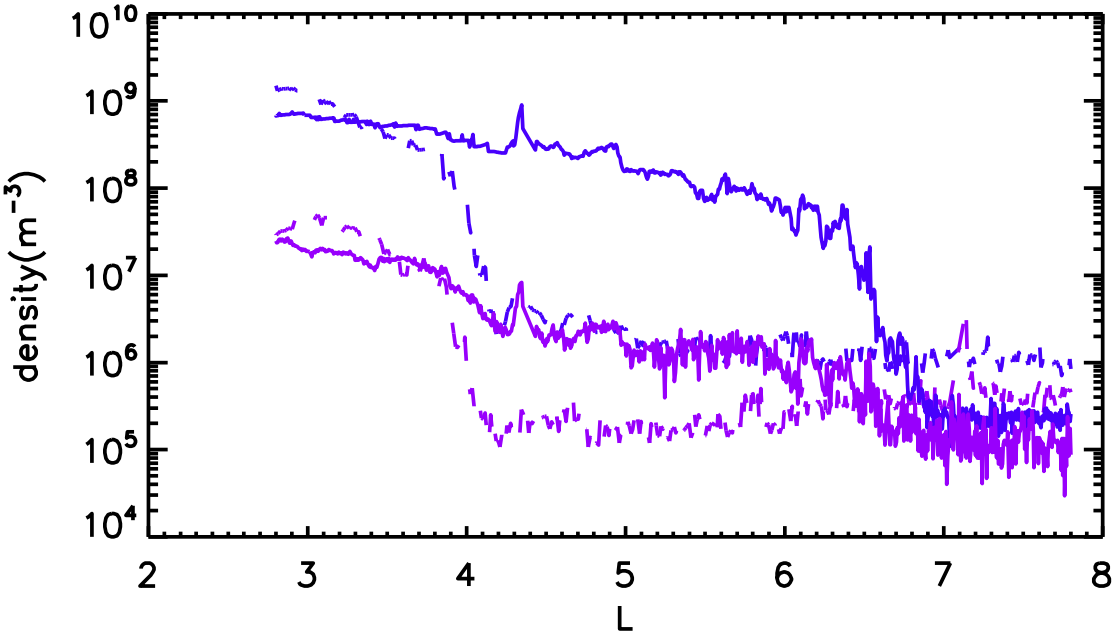

Fig. 11. The measured density of H^+ (blue) and He^+ (magenta) vs. L on March 7 and 9, 1968.
March 7, 1968 dashed lines - after the small magnetic disturbance
March 9, 1968 solid lines - the recovery phase

Results on comparison of the plasmapause location in H^+ and He^+ (Figure 7) showed some outliers. The most noticeable outlier belongs to the measurement on the 9 March 1968 (Figure 11). This measurement was realiyed in the recovery phase after a small geomagnetic disturbance. The plasmapause in H^+ was determined at L=6.4 but plasmapause in He^+ had two steps and the inner step had L=3.8 almost exactly as the plasmapause in H^+ two days ago (on 7 March 1968). We interpret this as a result of different recovery speed in H^+ and He^+. Similar finding was also discussed in Obana et al., 2010.

The last but not least result concerns density in the inner edge of plasmapause compared for corrected and uncorrected data (Figure 10). After the correction the lowest observed density is about 130 cm^{-3} which refers in the worst case to an altitude of about 4000 km (Figure 5). Tu et al. (2003) compared density along the field line for IMAGE/RPI and FLIP. The ratio of the density at the equator and at middle latitudes at about 4000 km was typically about 2. From it we can estimate that the density in the worst case from Figure 10b can shift from 130 cm^{-3} to about 60 cm^{-3}, which is still above the IMAGE EUV threshold.

7. Acknowledgements

We are grateful to the NASA GSFC's NSSDC for archivation of old OGO-5 ion mass spectrometer data on tapes and their restoration to IBM PC compatible ASCII format.
Works on this study was supported by following grants: LH11123 of MSMT of the Czech Republic, ...

References

Angerami, J. J., J. O. Thomas, 1964. Studies of planetary atmospheres, 1, The distribution of electrons and ions in the earth's exosphere, J. Geophys. Res., 69, 4537.

Balan N., K.-I. Oyama, G.J. Bailey, and T.Abe, 1996. Plasmasphere electron temperature profiles and the effects of photoelectron trapping and an equatorial high-altitude heat source, J. Geophys. Res., 101, A10, 21,689-21,696.

D. Bilitza and Reinisch, B., International Reference Ionosphere 2007: Improvements and new parameters, J. Adv. Space Res., 42, #4, 599-609, doi:10.1016/j.asr.2007.07.048, 2008.

D. Bilitza, L.-A. McKinnell, B. Reinisch, and T. Fuller-Rowell, The International Reference Ionosphere (IRI) today and in the future, J. Geodesy, 85:909-920, DOI 10.1007/s00190-010-0427-x, 2011.

Bilitza, D., V. Truhlik, P. Richards, T. Abe, L. Triskova, 2007. Solar cycle variations of mid-latitude electron density and temperature: satellite measurements and model calculations, Adv. Space Res., 39 (2007), pp. 779–789.

Carpenter, D. L., 1966. Whistler studies of the plasmapause in the magnetosphere, 1, Temporal variations in the position of the knee and some evidand some evidence on plasma near the knee, J. Geophys. Res., 71, 693.

Carpenter, D. L., and R. R. Anderson (1992), An ISEE/Whistler model of equatorial electron-density in the magnetosphere, J. Geophys. Res., 97(A2), 1097–1108, doi:10.1029/91JA01548.

Chandler, M. O., Ponthieu, J. J., Cravens, T. E., Nagy, A. F., Richards, P. G., 1987. Model calculations of minor ion populations in the plasmasphere, J. Geophys. Res., 92(A6), 2156-2202, doi:10.1029/JA092iA06p05885.

Chappell, C. R., K. K. Harris, and G. W. Sharp (1970), A study of the influence of magnetic activity on the location of the plasmapause as measured by OGO 5, J. Geophys. Res., 75(1), 50–56, doi:10.1029/JA075i001p00050

Craven, P. D., D. L. Gallagher, and R. H. Comfort (1997), Relative concentration of He+ in the inner magnetosphere as observed by the DE 1 retarding ion mass spectrometer, J. Geophys. Res., 102(A2), 2279–2289, doi:10.1029/96JA02176.

F. Darrouzet, D. L. Gallagher, N. André, D. L. Carpenter, I. Dandouras, P. M.E. Décréau, J. De Keyser, R. E. Denton, J. C. Foster, J. Goldstein, M. B. Moldwin, B. Reinisch, B.R. Sandel, J. Tu, 2009a. Plasmaspheric Density Structures and Dynamics: Properties Observed by the CLUSTER and IMAGE, Missions, Space Sci Rev., 145: 55–106, DOI 10.1007/s11214-008-9438-9

Darrouzet F., J. De Keyser, V. Pierrard, 2009b. The Earth's Plasmasphere: A CLUSTER and IMAGE Perspective, Springer-Verlag New York Inc., ISBN 10: 144191322X / ISBN 13: 9781441913227.

Darrouzet, F., and De Keyser, J., 2012. The dynamics of the plasmasphere: Recent results, J. Atmos. Sol.-Terr. Phys., 99, 53-60.

Decreau P.M.E., D. Carpenter, C. R. Chappell, R. H. Comfort, J. Green, R. C. Olsen, J.H. Waite Jr. (1986), Latitudinal plasma distribution in the dusk plasmaspheric bulge: Refilling phase and quasi-equilibrium state. J. Geophys. Res. 91(A6), 6929–6943.

Fox, J. L., and K. Y. Sung (2001), Solar activity variations of the Venus thermosphere/ionosphere, J. Geophys. Res., 106, 21,305–21,335.

Goldstein, J., B. R. Sandel, M. F. Thomsen, M. Spasojevic´, and P. H. Reiff (2004), Simultaneous remote sensing and in situ observations of plasmaspheric drainage plumes, J. Geophys. Res., 109, A03202, doi:10.1029/2003JA010281.

Harris K.K. and Sharp G.W., 1969. OGO-V Ion Spectrometer, IEEE TRANSACTIONS ON GEOSCIENCE ELECTRONICS, VOL. GE-7, NO. 2, APRIL 1969.

Hedin, A. E. (1987), MSIS-86 thermosphere model, J. Geophys. Res., 92, 4649–4662.

Horwitz, J. L., L. H. Brace, R. H. Comfort, C. R. Chappell, 1986. Dual spacecraft measurements of plasmasphere-ionosphere coupling, J. Geophys. Res., 9111, 203.

J. L. Horwitz, R. H. Comfort ,P . G. Richards, M . O. Chandler, C . R. Chappell, P. Anderson, W. B. Hanson, and L. H. Brace, 1990. Plasmasphere-Ionosphere Coupling 2. Ion Composition Measurement at Plasmaspheric and Ionospheric Altitudes and Comparison With Modeling Results, J. Geophys. Res., 95, A6, 7949-7959.

Itikawa, Y. (1975), Electron-ion energy transfer rate, J. Atmos. Terr. Phys., 37, 1601–1602.

Krall J., and Huba J.D., 2013. SAMI3 simulation of plasmasphere refilling, Geophys. Res. Lett., 40, 2484-2488, doi:10.1002/grl.50458.

Kotova G.A., V. V. Bezrukikh, M. I. Verigin, O. S. Akentieva, and J. Smilauer, 2008. Study of Notches in the Earth's Plasmasphere Based on Data of the MAGION-5 Satellite, Cosmic Research, 2008, Vol. 46, No. 1, pp. 15–24

Lemaire J.F., K.I. Gringauz, The Earth's Plasmasphere (Cambridge University Press, New York, 1998).

Nagy, A., and P. Banks (1970), Photoelectron fluxes in the ionosphere, J. Geophys. Res., 75, 6260–6270.

Picone, J. M., A. E. Hedin, D. P. Drob, and A. C. Aikin (2002), NRLMSISE-00 empirical model of the atmosphere: Statistical comparisons and scientific issues, J. Geophys. Res., 107(A12), 1468, doi:10.1029/2002JA009430.

Pierrard V., J. Goldstein, N. André, V. K. Jordanova, G.A. Kotova, J. F. Lemaire, M. W. Liemohn, H. Matsui, 2009. Recent Progress in Physics-Based Models of the Plasmasphere, Space Sci Rev., 145: 193–229, DOI 10.1007/s11214-008-9480-7.

Newberry, I.T., Comfort, R.H., Richards, P.G., Chappell, C. R., 1989. Thermal He+ in the plasmasphere: Comparison of observations with numerical calculations, J. Geophys. Res., 15265-15276, doi:10.1029/JA094iA11p15265.

Obana, Y., G. Murakami, I. Yoshikawa, I. R. Mann, P. J. Chi, and M. B. Moldwin (2010), Conjunction study of plasmapause location using ground-based magnetometers, IMAGE-EUV, and Kaguya-TEX data, J. Geophys. Res., 115, A06208, doi:10.1029/2009JA014704.

Radicella S.M., 2009. The NeQuick model genesis, uses and evolution, Annals of Geophysics, Vol. 52, No. 3, 417-422.

Richards, P. G. (1986), Thermal electron quenching of N(2D): Consequences for the ionospheric photoelectron flux and the thermal electron temperature, Planet. Space Sci., 34, 689–694.

Richards, P. G., J. A. Fennelly, and D. G. Torr (1994), EUVAC: A solar EUV flux model for aeronomic calculations, J. Geophys. Res., 99, 8981–8992.

Richards, P. G., 2001. Seasonal and solar cycle variations of the ionospheric peak electron density: Comparison of measurement and models, J. Geophys. Res., 106, 12,803–12,819.

Richards, P. G., T. N. Woods, and W. K. Peterson (2006), HEUVAC: A new high resolution solar EUV proxy model, Adv. Space Res., 37, 315–322, doi:10.1016/j.asr.2005.06.031.

Richards, P. G., D. Bilitza, and D. Voglozin, 2010. Ion density calculator (IDC): A new efficient model of ionospheric ion densities, Radio Sci., 45, RS5007, doi:10.1029/2009RS004332.

Sandel, B. R., J. Goldstein, D. L. Gallagher, and M. Spasojević (2003), Extreme ultraviolet imager observations of the structure and dynamics of the plasmasphere, Space Sci. Rev., 109, 25, doi:10.1023/B:SPAC.0000007511.47727.5b.

Schunk, R. W., and A. F. Nagy (1978), Electron temperatures in the F region of the ionosphere: Theory and observations, Rev. Geophys., 16, 355–399.

Storey, L.R.O., 1953. An investigation of whistling atmospherics. Philos Trans. R. Soc. London, Ser. A, 246, 113.

Torr, M. R., D. G. Torr, P. G. Richards, and S. P. Yung (1995), Mid- and low-latitude model of thermospheric emissions, 1, O+(2P) 7320 Å and N2(2P) 3371 Å, J. Geophys. Res., 95, 21,147–21,168.

Triskova, L., V. Truhlik, J. Smilauer (2003), An empirical model of ion composition in the outer ionosphere, Adv. Space Res., 31 (3), 653-663, doi:10.1016/S0273-1177(03)00040-1.

Truhlik, V., L. Triskova, J. Smilauer (2004), New advances in empirical modeling of ion composition in the outer ionosphere, Adv. Space Res., 33(6), 844-849, doi:10.1016/j.asr.2003.06.006.

Tu, J.-N., J. L. Horwitz, P. Song, X.-Q. Huang, B. W. Reinisch, and P. G. Richards, 2003. Simulating plasmaspheric field-aligned density profiles measured with IMAGE/RPI: Effects of plasmasphere refilling and ion heating, J. Geophys. Res., 108 (A1), 1017, doi:10.1029/2002JA009468.